Short-Lived Quinonoid Species from 5,6-Dihydroxyindole Dimers en Route to Eumelanin Polymers: Integrated Chemical, Pulse Radiolytic, and Quantum Mechanical Investigation

ARTICLE *in* JOURNAL OF THE AMERICAN CHEMICAL SOCIETY · JANUARY 2007

Impact Factor: 12.11 · DOI: 10.1021/ja0650246 · Source: PubMed

J|A|C|S
ARTICLES
Published on Web 11/11/2006

Short-Lived Quinonoid Species from 5,6-Dihydroxyindole Dimers en Route to Eumelanin Polymers: Integrated Chemical, Pulse Radiolytic, and Quantum Mechanical Investigation

Alessandro Pezzella,[†] Lucia Panzella,[†] Orlando Crescenzi,[‡] Alessandra Napolitano,[†] Suppiah Navaratman,[§,||] Ruth Edge,[§,⊥] Edward J. Land,[⊥] Vincenzo Barone,*[,‡] and Marco d'Ischia*[,†]

Contribution from the Departments of Organic Chemistry and Biochemistry and of Chemistry and INSTM, University of Naples Federico II, Via Cintia, I-80126 Naples, Italy, and Lennard-Jones Laboratories, School of Physical & Geographical Sciences, Keele University, Staffordshire ST5 5BG, Free Radical Research Facility, Daresbury Laboratory, Warrington, Cheshire WA4 4AD, and BioSciences Research Institute, University of Salford, Salford M5 4WT, United Kingdom

Received July 24, 2006; E-mail: baronev@unina.it; dischia@unina.it

Abstract: The transient species formed by oxidation of three dimers of 5,6-dihydroxyindole (**1**), a major building block of the natural biopolymer eumelanin, have been investigated. Pulse radiolytic oxidation of 5,5′,6,6′-tetrahydroxy-2,4′-biindolyl (**3**) and 5,5′,6,6′-tetrahydroxy-2,7′-biindolyl (**4**) led to semiquinones absorbing around 450 nm, which decayed with second-order kinetics ($2k = 2.8 \times 10^9$ and 1.4×10^9 M^{-1} s^{-1}, respectively) to give the corresponding quinones (500−550 nm). 5,5′,6, 6′-Tetrahydroxy-2,2′-biindolyl (**2**), on the other hand, furnished a semiquinone ($\lambda_{max} = 480$ nm) which disproportionated at a comparable rate ($2k = 3 \times 10^9$ M^{-1} s^{-1}) to give a relatively stable quinone ($\lambda_{max} = 570$ nm). A quantum mechanical investigation of *o*-quinone, quinonimine, and quinone methide structures of **2**−**4** suggested that oxidized **2**−**4** exist mainly as 2-substituted extended quinone methide tautomers. Finally, an oxidation product of **3** was isolated for the first time and was formulated as the hydroxylated derivative **5** arising conceivably by the addition of water to the quinone methide intermediate predicted by theoretical analysis. Overall, these results suggest that the oxidation chemistry of biindolyls **2**−**4** differs significantly from that of the parent **1**, whereby caution must be exercised before concepts that apply strictly to the mode of coupling of **1** are extended to higher oligomers.

Introduction

The oxidative polymerization of 5,6-dihydroxyindole (**1**) and related tyrosine-derived metabolites is a central, most elusive process in the biosynthesis of eumelanins, the characteristic pigments responsible for the dark colorations of human skin, hair, and eyes.[1] Eumelanins exhibit marked insolubility in all solvents and are characterized by a unique set of physicochemical properties, including broad-band monotonic absorption in the UV−vis range,[2] persistent free radical centers,[3] metal- and drug-binding properties,[4−6] susceptibility to redox changes,[7] strong excited-state−phonon coupling,[8] and amorphous electrical switch behavior.[9] The socioeconomic and biomedical importance of eumelanins stems from their relevance to racial pigmentation, skin photoprotection, sun tanning, and pigmentary disorders, such as albinism, vitiligo, and melanoma.[10] Despite intense research efforts spanning over nearly a century,[11] the eumelanin structure remains poorly understood, because of the chemical heterogeneity and the lack of well-defined physico-

[†] Department of Organic Chemistry and Biochemistry, University of Naples Federico II.
[‡] Department of Chemistry and INSTM, University of Naples Federico II.
[§] Daresbury Laboratory.
[||] University of Salford.
[⊥] Keele University.

(1) Prota, G. *Melanins and Melanogenesis*; Academic Press: San Diego, CA, 1992.
(2) Nighswander-Rempel, S. P.; Riesz, J.; Gilmore, J.; Bothma, J. P.; Meredith, P. *J. Phys. Chem. B* **2005**, *109*, 20629−20635.
(3) Seagle, B. L.; Rezai, K. A.; Gasyna, E. M.; Kobori, Y.; Rezaei, K. A.; Norris, J. R., Jr. *J. Am. Chem. Soc.* **2005**, *127*,11220−11221.
(4) Bridelli, M. G.; Ciati, A.; Crippa, P. R. *Biophys. Chem.* **2006**, *119*, 137−145.
(5) Hong, L.; Liu, Y.; Simon, J. D. *Photochem. Photobiol.* **2004**, *80*, 477−481.
(6) Samokhvalov, A.; Liu, Y.; Simon, J. D. *Photochem. Photobiol.* **2004**, *80*, 84−88.
(7) Ye, T., Hong, L., Garguilo, J., Pawlak, A., Edwards, G. S.; Nemanich, R. J.; Sarna, T.; Simon, J. D. *Photochem. Photobiol.* **2006**, *82*, 733−777.
(8) Meredith, P; Riesz, J. *Photochem. Photobiol.* **2004**, *79*, 211−216.
(9) McGinness, J.; Corry, P.; Proctor, P. *Science* **1974**, *183*, 853−855.
(10) Prota, G.; d'Ischia, M.; Napolitano, A. In *The Pigmentary System: Its Physiology and Pathophysiology*; Nordlund, J. J., Boissy, R. E., Hearing, V. J., King, R. A., Ortonne, J. P., Eds.; Oxford University Press: New York, 1998; Chapter 24, pp 307−332.
(11) Prota, G. *Fortschr. Chem. Org. Naturst.* **1995**, *64*, 93−148.

10.1021/ja0650246 CCC: $33.50

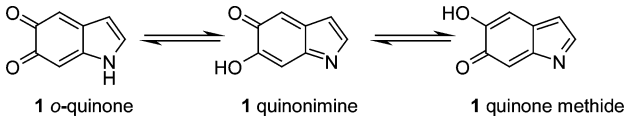

Figure 1. Tautomeric equilibria of the quinone of **1**.

chemical properties, preventing successful application of modern spectroscopic techniques.

The role of the 5,6-dihydroxyindoles as eumelanin building blocks has been known since 1927[12] and is illustrated by their rapid conversion to black insoluble pigments following exposure to oxidizing enzymes, UV radiation, and chemical oxidants or even on standing at neutral physiologic pH.[12] Interest in 5,6-dihydroxyindole oxidation is also spurred by the prospects of preparing polymeric materials with controlled structural properties and functionalities for high-technology applications such as biosensors and photovoltaics.[13]

Chemical efforts to elucidate the early species formed in the oxidation of **1** led to the isolation of a collection of dimers and trimers which revealed a prevalent mode of coupling of the indole monomer through the 2-, 4-, and 7-positions, as shown by the structures of the dimers **2**−**4**.[14]

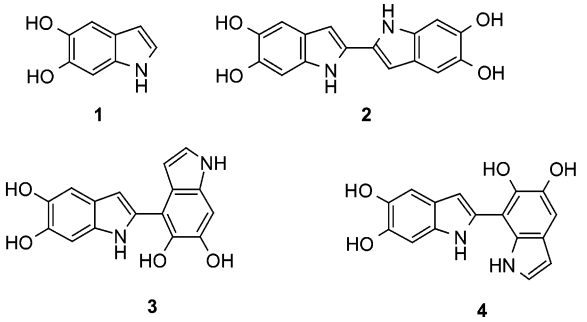

The mechanism of indole dimerization is uncertain, but a catechol−quinone interaction seems the most likely route on the basis of product structures and quinone trapping experiments with sulfur nucleophiles.[15,16]

Valuable insights have also derived from the application of pulsed radiation techniques. One-electron oxidation of **1** in aqueous solution at pH 7.4, using the azide radical as an oxidant, leads to an initial transient spectrum with peaks at 330 and 490 nm and a shoulder at 360 nm,[17] ascribed to an oxygen-centered radical with significant electron delocalization over the nitrogen ring.[18] This semiquinone may decay via disproportionation to give a mixture of *o*-quinone, quinone methide, and quinonimine species (Figure 1). It was argued on the basis of a peak in the 430 nm region that the initial product observed after 5,6-dihydroxyindole semiquinone disproportionation is the quinone methide.[19]

However, quantum mechanical computations[20] by methods rooted in the density functional theory (DFT) predicted 5,6-indole quinone in aqueous solution to exist almost exclusively as a single *o*-quinone tautomer with no significant absorption in the range 400−600 nm, suggesting that second-order decay of semiquinone may involve other pathways, e.g., dimerization, in addition to disproportionation. Separate calculations have also been performed on the semiquinone and the quinone of **1**,[21] as well as on dimers[22] and hypothetical oligomer structures.[23] Recently, it has been suggested[23b] that dihydroxyindoles could also form "square" dimers (with two parallel or antiparallel indole units) and that such dimers, featuring two intermonomer bonds, are stable with respect to dimers with a single bond. However, experimental evidence supporting their actual formation is so far lacking. The calculated oligomeric spectra suggested a eumelanin structure consisting of oligomeric indole quinone substructures arranged as stacked graphitic-like sheets.[24,25]

Virtually nothing is known on the oxidation chemistry of oligomers of **1**: all attempts to investigate the species formed beyond the dimer level were unsuccessful due to the complex mixtures of products formed and their instability and insolubility. A significant goal in this area would therefore be to identify the first species generated from oxidation of the oligomer intermediates, to determine their spectroscopic properties and kinetics of decay, and to map their patterns of reactivity in comparison with the parent heterocycle **1**, in order to delineate main reaction channels and to predict their relative importance.

As an initial step toward this goal, we have improved previous procedures for the preparation of the three major dimers of **1**, viz., **2**−**4**, and have investigated for the first time the absorption properties of the transient semiquinones and quinones generated by pulse radiolytic oxidation of **2**−**4**.

Computational analysis and simulation of electronic absorption spectra of an array of candidate products allowed structural assignment to the transient quinonoid species from oxidation of these dimers.

Results and Discussion

Preparation of Dimers 2−4. Although dimers **2**−**4** were first described two decades ago by biomimetic oxidation of **1**,[14,26] their preparation even on a milligram scale remains a most difficult task. No concise organic synthesis for the construction of the tetrahydroxybiindolyl systems has been described so far, and oxidative coupling of **1** is to date the only viable option. For the purposes of the present study, optimized procedures for preparing small amounts of dimers **2**−**4** in pure form by oxidation of **1** were set up, involving use of horseradish peroxidase (HRP)/H_2O_2 in phosphate buffer at pH 7. Under these conditions dimers **3** and **4** were obtained at a molar ratio of 1.6 and could be isolated as acetyl derivatives in better yields compared to those of previous procedures.[14]

In the course of those studies, we found that addition of organic solvents such as methanol, ethanol, THF, or acetone

(12) Raper, H. S. *Biochem. J.* **1927**, *21*, 89−96.
(13) de Albuquerque, J. E.; Giacomantonio, C.; White, A. G.; Meredith, P. *Eur. Biophys. J.* **2006**, *35*, 190−195.
(14) d'Ischia, M.; Napolitano, A.; Tsiakas, K. Prota, G. *Tetrahedron* **1990**, *46*, 5789−5796.
(15) d'Ischia, M.; Napolitano, A.; Prota, G. *Tetrahedron* **1987**, *43*, 5351−5356.
(16) d'Ischia, M.; Napolitano, A.; Pezzella, A.; Land, E. J.; Ramsden,C. A. Riley, P. A. *Adv. Heterocycl. Chem.* **2005**, *89*, 1−63.
(17) Lambert, C.; Chacon, J. N.; Chedekel, M. R.; Land, E. J.; Riley, P. A.; Thompson, A.; Truscott, T. G. *Biochim. Biophys. Acta* **1989**, *993*, 12−20.
(18) Felix, C. C.; Sealy, R. C. *Photochem. Photobiol.* **1981**, *34*, 423−429.
(19) Al-Kazwini, A.T.; O'Neill, P.; Adams, G. E.; Cundall, R.B.; Lang, G.; Junino, B. *J. Chem. Soc., Perkin Trans. 2* **1991**, 1941−1945.
(20) Il'ichev, Y. V.; Simon, J. D. *J. Phys. Chem.* **2003**, *107*, 7162−7171.
(21) Powell, B. J.; Baruah, T.; Bernstein, N.; Brake, K.; McKenzie, R. H.; Meredith, P.; Pederson, M. R. *J. Chem. Phys.* **2004**, *120*, 8608−8615.
(22) Stark, K. B.; Gallas, J. M.; Zajac, G. W.; Eisner, M.; Golab, J. T. *J. Phys. Chem.* **2003**, *107*, 3061−3067.
(23) (a) Stark, K. B.; Gallas, J. M.; Zajac G. W.; Eisner, M.; Golab, J. T. *J. Phys. Chem.* **2003**, *107*, 11558−11562. (b) Tran, M. L.; Powell, B. J.; Meredith, P. *Biophys. J.* **2006**, *90*, 743.
(24) Cheng, J.; Moss, S. C.; Eisner, M. *Pigm. Cell Res.* **1994**, *7*, 263−273.
(25) Zajac, G. W.; Gallas, J. M.; Alvarada-Swaisgood, A. E. *J. Vac. Sci. Technol., B* **1994**, *12*, 1512.
(26) Napolitano, A.; Corradini, M. G.; Prota, G. *Tetrahedron Lett.* **1985**, *26*, 2805−2808.

subverted the **3**:**4** product ratio in favor of the latter dimer: for example, oxidation of **1** in acetone/0.1 M phosphate buffer, pH 7 (3:1, v/v), resulted in a 3 times higher formation yield of **4** (12% molar yield) with respect to **3**.

Formation of **2** is known to depend on transition-metal catalysis.[26] Accordingly, an optimized procedure for the preparation of **2** was set up which involved HRP/H_2O_2 oxidation of **1** in β-hydroxy-4-(2-hydroxyethyl)-1-piperazinepropanesulfonic acid (HEPPSO) buffer at pH 7.0 in the presence of 2.0 equiv of Ni^{2+}, indicating that metal ions may exert a directional effect by chelate formation with the *o*-diphenolic moiety of **1**. Under these conditions, dimers **3** and **4** were not formed in appreciable amounts. Interestingly, acetone or ethanol virtually suppressed the metal-induced formation of **2**, suggesting that the chelate is disrupted in the presence of organic solvents. It is very likely that metal binding affects the equilibrium between the tautomeric forms of the constituent monomers, but how this happens could not be assessed at the present level of investigation and goes beyond the scope of this study.

Pulse Radiolysis. Pulse radiolysis was carried out as described previously.[27,28] Generation of the oxidizing species $Br_2^{\bullet-}$ was achieved by irradiating N_2O-saturated solutions of 0.5 M KBr. Under such conditions, $Br_2^{\bullet-}$ radicals are formed within 0.1 μs after the radiation pulse according to the following equations:

$$H_2O \rightsquigarrow e^-_{aq} + OH^\bullet$$

$$e^-_{aq} + N_2O + H_2O \rightarrow OH^\bullet + N_2 + OH^-$$

$$OH^\bullet + Br^- \rightarrow OH^- + Br^\bullet$$

$$Br^\bullet + Br^- \rightarrow Br_2^{\bullet-}$$

Because dimers **2**−**4** were obtained and stored as the tetraacetyl derivatives, an efficient deacetylation procedure compatible with the experimental conditions for pulse radiolysis was required. This procedure was set up using 5,6-diacetoxyindole as a reference compound and involved treatment of the acetylated indole under a N_2O atmosphere in 0.025 M trisodium phosphate containing 0.5 M KBr, followed by addition of sodium dihydrogen phosphate up to pH 7.0. To test the efficiency of the procedure and to ascertain whether the experimental conditions used in the present study allowed comparison of data with previous results,[17] 5,6-diacetoxyindole (0.15 mM) was deacetylated by the above procedure and subjected to pulse radiolysis. The results were compared with those obtained in another series of experiments using the parent **1** at the same concentration and in previous studies with the azide radical as the oxidizing agent.[17] In both cases, a similar semiquinone chromophore was obtained displaying a distinct maximum at 480 nm, as reported,[17] which changed into a species with a less defined chromophore (460 nm with accompanying broad shoulders in the 410−490 nm range) decreasing monotonically with increasing wavelength.

On the basis of these preliminary experiments, pulse radiolytic one-electron oxidation of dimers **2**−**4** was carried out by irradiation of a N_2O-saturated 0.15 mM solution of the substrate that had been deacetylated under N_2O just prior to irradiation. The series of successive transient absorption spectra thus obtained from **2**−**4** are shown in Figures 2−4, respectively. In each case, the first transient spectrum was recorded at such a time that the buildup of initial radical absorption was complete and that subsequent decay had not proceeded to any significant extent.

Figure 2 shows that the initial product from **2** completely formed 130 μs after the pulse was the semiquinone, with a sharp maximum around 480 nm and a broad, less intense band centered at 650 nm. The rate constant for the reaction of **2** with

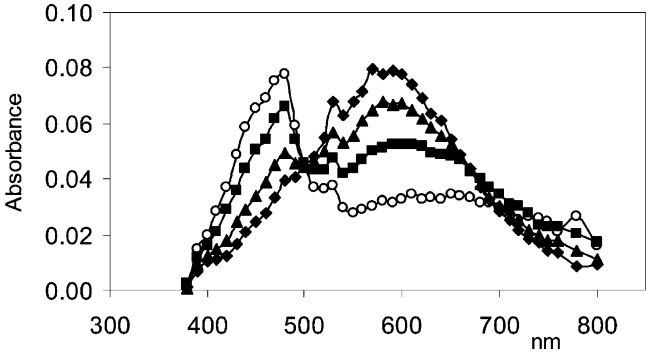

Figure 2. Changes in absorption at various times after pulse radiolysis of a N_2O-saturated aqueous solution of dimer **2** (1.5×10^{-4} M) in 0.5 M KBr/7.0×10^{-2} M phosphate buffer, pH 7.0: (○) 130 μs; (■) 480 μs; (▲) 1.38 ms; (◆) 4.4 ms.

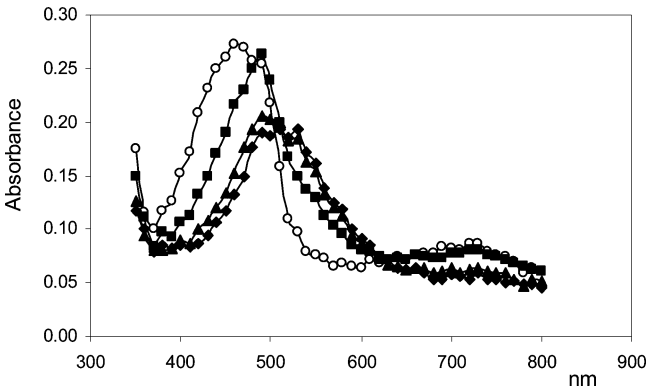

Figure 3. Changes in absorption at various times after pulse radiolysis of a N_2O-saturated aqueous solution of dimer **3** (1.5×10^{-4} M) in 0.5 M KBr/7.0×10^{-2} M phosphate buffer, pH 7.0: (○) 14 μs; (■) 102 μs; (▲) 402 μs; (◆) 866 μs.

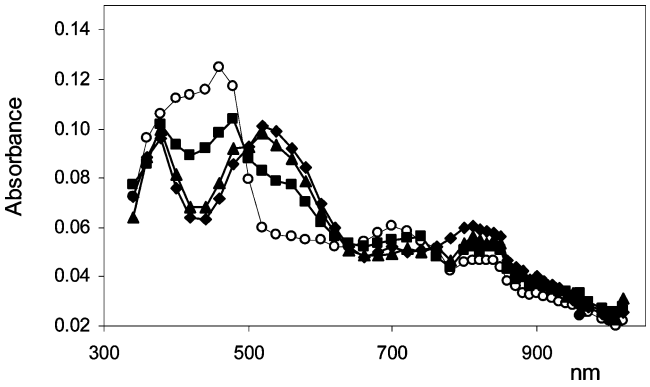

Figure 4. Changes in absorption at various times after pulse radiolysis of a N_2O-saturated aqueous solution of dimer **4** (1.5×10^{-4} M) in 0.5 M KBr/7.0×10^{-2} M phosphate buffer, pH 7.0: (○) 18 μs; (■) 100 μs; (▲) 402 μs; (◆) 866 μs.

(27) Napolitano, A.; Di, Donato, P.; Prota, G.; Land, E. J. *Free Radical Biol. Med.* **1999**, *27*, 521−528.
(28) Land, E. J.; Ramsden, C. A.; Riley, P. A. *J. Photochem. Photobiol., B* **2001**, *64*, 123−135.

$Br_2^{\bullet-}$ was estimated to be $k = 9 \times 10^7$ M^{-1} s^{-1}. The extinction coefficient of the semiquinone at 480 nm was calculated to be 4.0×10^4 M^{-1} cm^{-1}.

The transient species decayed by second-order kinetics ($2k = 3 \times 10^9$ M^{-1} s^{-1}) to a species with a broad band centered at 570 nm ($\epsilon = 9.0 \times 10^4$ M^{-1} cm^{-1}) and a shoulder at 520 nm. The isosbestic point at 500 nm denoted direct conversion of the first species to the bathochromically shifted chromophore. It may be noted that the spectrum of the relatively stable species formed from the decay of the semiquinone of **2** is closely similar to that of melanochrome observed in the metal-catalyzed oxidation of **2**.[26] Indeed, the species may well be identical.

Figures 3 and 4 indicate that **3** and **4** behaved quite differently from **2**. Dimer **3** gave a semiquinone ($\lambda_{max} = 460$ nm, $\epsilon = 11700$ M^{-1} cm^{-1}) with a formation rate constant $k = 1.8 \times 10^9$ M^{-1} s^{-1}. The semiquinone(s) apparently decayed with second-order kinetics ($2k = 2.8 \times 10^9$ M^{-1} s^{-1}), resulting in the generation of species with broad bands at 490 nm ($\epsilon = 17700$ M^{-1} cm^{-1}) and at 530 nm ($\epsilon = 15900$ M^{-1} cm^{-1}). Dimer **4** gave a semiquinone (formation rate constant $k = 2.2 \times 10^9$ M^{-1} s^{-1}) with a broader, seemingly split band ($\lambda_{max} = 430$ nm, $\epsilon = 8.6 \times 10^3$ M^{-1} cm^{-1}, and 480 nm, $\epsilon = 8.1 \times 10^3$ M^{-1} cm^{-1}). The semiquinone(s) decayed with second-order rate constants $2k = 1.4 \times 10^9$ M^{-1} s^{-1} measured at 480 nm and $2k = 2.1 \times 10^9$ M^{-1} s^{-1} determined at 430 nm. Concomitant to semiquinone decay, a chromophore developed with a broad maximum centered around 530 nm. If it is assumed that a single semiquinone species is responsible for the bands at 420 and 480 nm, then the extinction coefficient of the quinone can be calculated to be 11100 M^{-1} cm^{-1} at 530 nm taking as reference the semiquinone band at 480 nm. If there is more than one quinone, such a calculation is invalid. Overall, these pulse radiolysis studies suggested that oxidation of **2**−**4** leads to the generation of semiquinone intermediates which decay by a bimolecular process. This may consist of either disproportionation, to give two-electron oxidation products generically referred to as "quinones", or dimerization, to afford tetraindolyl species. To address this issue, a theoretical investigation of the main tautomeric forms of quinones from dimers **2**−**4** was undertaken.

Theoretical Studies and Simulated Electronic Absorption Spectra of Biindolyl Quinone Tautomers. Pairs of syn-periplanar (*sp*) and anti-periplanar (*ap*) rotamers can be envisaged for the *o*-quinone, quinone methide, and quinonimine tautomers of dimers **2**−**4**, depending on the orientation of the indole rings around the single bond, whereas two geometrical isomers (*E* and *Z*) are possible for the extended forms. To determine which of these structures may be a plausible candidate for the observed two-electron oxidation products of the dimers, all tautomeric quinones of dimers **2**−**4** were geometry-optimized in vacuo at the PBE0/6-31+G(d,p) level of theory.[29] For each dimer, all structures that were within ca. 15 kcal mol^{-1} from the minimum-energy structure were also optimized using the polarizable continuum model (PCM)[30] to simulate the aqueous environment; the absorption spectra of all the energetically relevant species were computed using the time-dependent DFT (TDDFT)[31] approach both in vacuo and in aqueous solution, using the large 6-311++G(2d,2p) basis set. Previously,[22] a DFT analysis of five oxidized 5,6-dihydroxyindole dimers was reported, using both local density approximation (LDA) and generalized gradient approximation (GGA) functionals. In that study, however, only doubly quinonoid structures, viz., at an oxidation state two electrons higher than those described in the present study, were considered. In particular two conformers of a 3,7′-biindolyl system as yet devoid of experimental support were investigated.

For the purposes of the present study, we chose to use the "hybrid" PBE0 functional, which has been shown to provide quite satisfactory energies and geometries for a wide range of organic and biological systems,[32] as well as a rather accurate description of low-lying excited states.[33] To assess the performance of the selected DFT technique in predicting electronic absorption spectra of dimeric quinones, test calculations were carried out on simple benzoquinones/benzoquinone imines, and on indigo, a prototypical conjugated indole dimer. Overall, the results (see the Supporting Information) confirmed that the method chosen is capable of reproducing the UV−vis spectra of such chromophores with reasonable accuracy. Thus, for example, if one focuses on the most intense transitions, the predicted wavelength for *p*-benzoquinone in vacuo is 247 nm, to compare with an experimental value of 240 nm. For *p*-benzoquinonimine (in water) the computed transition is at 266 nm, while the experimental spectrum shows a split band with maxima at 260 and 254 nm. The related *N*-phenyl-*p*-benzoquinonimine in methanol has strong transitions at 490, 309, and 267 nm, in fair agreement with the experimental values of 448, 285, and 263 nm. A comparable error is obtained in the case of indigo (computed 570 nm, measured 600 nm).

The molecular structures of the main quinone tautomers for dimer **2** along with their relative energies are shown in Figure 5; a complete listing of the structures examined is presented in the Supporting Information.

DFT results suggest that the extended forms **2a** and **2b** are by far the most stable tautomers in the series. The structures that come next, namely, methides **2c** and **2d** in vacuo, and quinone **2g** in aqueous solution, are separated by several kilocalories per mole. Interestingly, in vacuo the *E* isomer **2b** is planar and slightly more stable than the *Z* isomer **2a**, in which the indole rings are twisted by 3.4°. However, in aqueous solution both isomers are planar and the *E* isomer is destabilized by ca. 1.1 kcal mol^{-1}. With respect to all other tautomers, the *o*-quinone tautomers feature one less intramolecular OH−O hydrogen bond. Thus, their relative stability increases signifi-

(29) Adamo, C.; Barone, V. *J. Chem. Phys.* **1999**, *110*, 6158−6170.
(30) (a) Miertus, S.; Scrocco, E.; Tomasi, J. *Chem. Phys.* **1981**, *55*, 117−129. (b) Cossi, M.; Scalmani, G.; Rega, N.; Barone, V. *J. Chem. Phys.* **2002**, *117*, 43−54. (c) Scalmani, G.; Barone, V.; Kudin, K. N.; Pomelli, C. S.; Scuseria, G. E.; Frisch, M. J. *Theor. Chem. Acc.* **2004**, *111*, 90−100.
(31) (a) Stratmann, R. E.; Scuseria, G. E.; Frisch, M. J. *J. Chem. Phys.* **1998**, *109*, 8218−8224. (b) Bauernschmitt, R.; Ahlrichs, R. *Chem. Phys. Lett.* **1996**, *256*, 454−464. (c) Casida, M. E.; Jamorski, C.; Casida, K. C.; Salahub, D. R. *J. Chem. Phys.* **1998**, *108*, 4439−4449. (d) Adamo, C.; Scuseria, G. E.; Barone, V. *J. Chem. Phys.* **1999**, *111*, 2889−2899.
(32) (a) Improta, R.; Barone, V. *J. Am. Chem. Soc.* **2004**, *126*, 14320−14321. (b) Benzi, C.; Improta, R.; Scalmani, G.; Barone, V. *J. Comput. Chem.* **2002**, *23*, 341−350. (c) Langella, E.; Rega, N.; Improta, R.; Crescenzi, O.; Barone, V. *J. Comput. Chem.* **2002**, *23*, 650−661. (d) Improta, R.; Mele, F., Crescenzi, O.; Benzi, C.; Barone, V. *J. Am. Chem. Soc.* **2002**, *124*, 7857−7865.
(33) (a) Jacquemin, D.; Wathelet, V.; Perpete, E. A. *J. Phys. Chem. A* **2006**, *110*, 9145−9152. (b) Preat, J.; Jacquemin, D.; Wathelet, V.; Andre, J.-M.; Perpete, E. A. *J. Phys. Chem. A* **2006**, *110*, 8144−8150. (c) Jacquemin, D.; Preat, J.; Wathelet, V.; Fontaine, M.; Perpete, E. A. *J. Am. Chem. Soc.* **2006**, *128*, 2072−2083. (d) Crescenzi, O.; Pavone, M.; De Angelis, F.; Barone, V. *J. Phys. Chem. B* **2005**, *109*, 445−453. (e) Aquilante, F.; Cossi, M.; Crescenzi, O.; Scalmani, G.; Barone, V. *Mol. Phys.* **2003**, *101*, 1945−1953. (f) Adamo, C.; Barone, V. *Chem. Phys. Lett.* **2000**, *330*, 152−160.

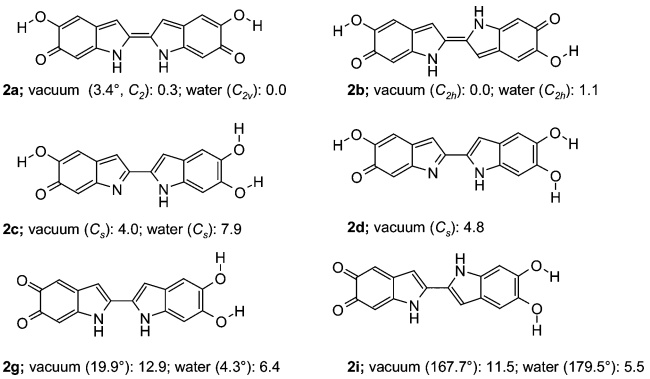

Figure 5. Structures and relative energies (kcal mol^{-1}) of several tautomers/conformers of **2**, computed at the PBE0/6-31+G(d,p) level in vacuo or in aqueous solution (PCM). In parentheses the inter-ring N−C−C−N dihedral angle (deg) and/or the symmetry group of the molecule is reported.

cantly in an aqueous environment: however, this effect is not sufficient to bring them close enough to the extended tautomers. In this dimer series, alternative conformations differing only in the orientation of the OH groups of a dihydroxyindole ring (e.g., **2c** and **2d**) were separately optimized. Within each pair, the conformer that orients the OH groups opposite to the nitrogen is invariably more stable; therefore, in the following only this conformation was considered, unless a preliminary inspection suggested that a different hydrogen bond pattern could arise in the other orientation. The above calculations therefore identified **2a** as the primary determinant of the measured absorption spectrum of **2** quinone, with only a minor contribution from the *E* isomer **2b** (ca. 15%, based on energy differences). Inclusion of harmonic vibrational contributions (see the Supporting Information) has a marginal impact on the overall picture. As a further check, single-point energies in aqueous solution were also computed at the MP2/6-31+G(d,p)/PCM level. While the separation between **2a** and **2b** is basically unaltered (see the Supporting Information), the energy gaps to other tautomers tend to become uniformly smaller; in particular, the contributions of **2c** (at 0.8 kcal mol^{-1}) and **2i** (at 1.1 kcal mol^{-1}) would become significant. Computed absorption spectra of these latter isomers, along with those of **2a** and **2b**, are given in Table 1. For a comparison of all computed absorption spectra with experimental data see the Supporting Information.

The computed absorption maxima of the main components **2a** and **2b** are quite close: around 500 nm in a vacuum and bathochromically shifted to ca. 550 nm in aqueous solution. These results are in qualitative agreement with the experimentally measured absorption maximum (570 nm) of the species formed by second-order decay of the transient semiquinone from **2**.

As to the nature of the bands in **2a** and **2b**, the DFT results (in vacuo) show that the 500 nm band corresponds to an allowed transition (501 nm, $f = 1.625$, and 512 nm, $f = 1.672$, respectively) with a strong HOMO → LUMO character. Longer wavelength transitions are also predicted, albeit with much lower oscillator strengths, corresponding essentially to HOMO − 1 → LUMO (575 nm, $f = 0.0005$, for **2a**, and 609 nm, $f = 0.014$, for **2b**) and HOMO − 2 → LUMO (549 nm, $f = 0.056$, for **2a**, and 571 nm, $f = 0.0000$, for **2b**) excitations. Except for the wavelength shifts hinted above, these results are essentially unaltered in aqueous solution.

The extended quinone methide structure **3a** (Figure 6), featuring a 2-substituted quinone methide moiety, was predicted to be the most stable of the tautomer structures under consideration for the "quinone" of dimer **3** (see the Supporting Information). In particular, the *Z* isomer was stabilized relative to the *E* isomer both in vacuo (by 5.1 kcal mol^{-1}) and in aqueous solution (by 3.1 kcal mol^{-1}), due to a hydrogen bond that forms between the indole NH group and the adjacent carbonyl oxygen atom. The next most stable tautomer was the *sp* 2-substituted

Table 1. Transition Wavelengths (nm) and Oscillator Strengths Computed at the PBE0/6-311+G(2d,2p)//PBE0/6-31+G(d,p) Level for the Most Stable Tautomers of **2**−**4** in Vacuo and/or in Aqueous Solution (PCM)[a]

	In Vacuo
2a	549 (0.056), 501 (1.625), 301 (0.015), 286 (0.032)
2b	609 (0.014), 512 (1.672)
2c	744 (0.014), 505 (0.146), 486 (0.702), 326 (0.104), 305 (0.029), 297 (0.464)
3a	884 (0.037), 492 (0.621), 343 (0.197), 332 (0.180), 284 (0.025)
3e	815 (0.062), 604 (0.013), 470 (0.679), 330 (0.093), 328 (0.208)
3i	756 (0.016), 511 (0.428), 338 (0.266), 305 (0.134), 294 (0.156), 289 (0.054)
4a	884 (0.073), 529 (0.483), 361 (0.299), 334 (0.165), 284 (0.011)
4e	819 (0.100), 584 (0.030), 504 (0.499), 352 (0.263), 331 (0.180)
4j	748 (0.013), 551 (0.332), 357 (0.357), 352 (0.035), 308 (0.071), 293 (0.104), 282 (0.054)
	In Aqueous Solution
2a	589 (0.160), 551 (1.742), 358 (0.018), 287 (0.070)
2b	659 (0.140), 558 (1.758)
2c	761 (0.051), 577 (0.021), 527 (1.123), 335 (0.149), 310 (0.032), 300 (0.394)
2g	828 (0.188), 547 (0.016), 522 (0.960), 332 (0.330), 319 (0.052), 292 (0.143)
2i	792 (0.158), 553 (0.115), 529 (0.871), 328 (0.323), 315 (0.127), 294 (0.093), 282 (0.047)
3a	956 (0.047), 655 (0.014), 534 (0.722), 357 (0.271), 340 (0.192), 291 (0.018), 282 (0.021)
3e	929 (0.071), 524 (0.781), 349 (0.214), 339 (0.185), 313 (0.017)
3i	817 (0.029), 763 (0.013), 552 (0.516), 353 (0.367), 314 (0.189), 301 (0.100), 294 (0.035)
3p	826 (0.081), 652 (0.049), 534 (0.377), 338 (0.256), 320 (0.086), 302 (0.107), 294 (0.169), 286 (0.077)
4a	897 (0.124), 557 (0.573), 395 (0.011), 373 (0.323), 338 (0.191), 295 (0.019)
4e	871 (0.153), 550 (0.594), 369 (0.322), 337 (0.209)
4j	818 (0.022), 766 (0.016), 577 (0.424), 366 (0.458), 311 (0.086), 297 (0.136), 283 (0.046)
4o	804 (0.077), 663 (0.019), 554 (0.309), 348 (0.314), 310 (0.111), 300 (0.114), 292 (0.196), 283 (0.020)
4q	779 (0.111), 670 (0.017), 557 (0.264), 347 (0.319), 310 (0.116), 298 (0.137), 293 (0.170)

[a] Only transitions with a wavelength above 280 nm and an oscillator strength above 0.010 are reported.

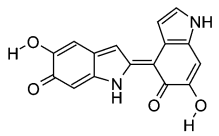

3a; vacuum (4.2°): 0.0; water (4.2°): 0.0

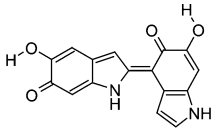

3e; vacuum (169.2°): 5.1; water (167.9°): 3.1

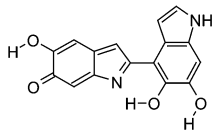

3i; vacuum (3.3°): 6.2; water (3.1°): 7.4

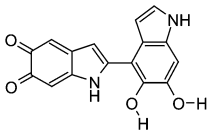

3p; vacuum (25.9°): 19.4; water (22.9°): 7.1

Figure 6. Structures and relative energies (kcal mol^{-1}) of several tautomers/conformers of **3**, computed at the PBE0/6-31+G(d,p) level in vacuo or in aqueous solution (PCM). In parentheses the inter-ring N−C−C−C(O) dihedral angle (deg) is reported.

quinone methide **3i**, in which a hydrogen bond can form between the nitrogen of the quinone methide ring and an OH group of the 4-substituted ring. This structure, however, was less favorable by 6.2 kcal mol^{-1} in a vacuum and by 7.4 kcal mol^{-1} in aqueous solution compared to **3a**, suggesting that it should not be present to an appreciable extent. The aqueous environment preferentially stabilizes the *o*-quinones (e.g., **3p**), but even so none of them reach a stability comparable to that of the extended tautomers. Again, single-point computations at the MP2/PCM level (see the Supporting information) showed a general flattening of the potential energy surface, but in this case no conformer comes close enough to the absolute minimum to become significantly populated.

The computed absorption spectra of quinones from **3** are given in Table 1. Calculations predicted for the most stable tautomer **3a** and for the *E* isomer **3e** in aqueous solution absorption maxima around 530 and 520 nm, respectively. Thus, both stability and excitation energy data suggest that tautomers **3a** and **3e** are responsible for the 530 nm band observed in the radiolysis experiments (Figure 3).

Since it is known that the PCM model can show limitations in the accurate description of highly specific solute−solvent interactions, the computed UV−vis spectrum of **3a** was used as a test case to evaluate the results of a cluster/PCM approach, which has proved very versatile in reproducing static and dynamic solvation effects.[33d,34] Thus, TDDFT/PCM computations were performed on some water adducts of **3a**, in which an explicit water molecule was hydrogen-bonded either to a carbonyl or to a hydroxyl group. However, in the wavelength region of interest the transitions turned out to be almost unchanged with respect to those computed with PCM alone (see the Supporting Information). Such insensitivity to the exact details of the hydrogen-bonding geometry is probably related to the nature of the transitions, which involve mainly strongly delocalized π orbitals.

From examination of the TDDFT results (in vacuo), the principal bands of **3a** and **3e** correspond to HOMO − 1 → LUMO excitations (**3a**, 492 nm, $f = 0.621$; **3e**, 470 nm, $f = 0.679$). In this case, the HOMO − 1 molecular orbital is mostly localized on the 4-substituted indole ring, while the LUMO is predominantly localized on the 2-substituted ring. The computed intensity of longer wavelength bands is at least a factor of 10 smaller: the HOMO → LUMO transition is predicted at 884 nm in **3a** (815 nm for **3e**), while the HOMO − 2 → LUMO transition would be at 634 nm (respectively 604 nm). The nature and ordering of these long-wavelength transitions are unchanged in aqueous solution, apart from wavelength shifts.

(34) (a) Barone, V.; Crescenzi, O.; Improta, R. *Quant. Struct.-Act. Relat.* **2002**, *21*, 105−118. (b) Cossi, M.; Crescenzi, O. *J. Chem. Phys.* **2003**, *118*, 8863−8872. (c) Pavone, M.; Benzi, C.; De, Angelis, F.; Barone, V. *Chem. Phys. Lett.* **2004**, *395*, 120−126. (d) Ciofini, I.; Adamo, C.; Barone, V. *J. Chem. Phys.* **2004**, *121*, 6710−6718.

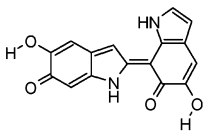

4a; vacuum (8.8°): 0.0; water (10.2°): 0.0

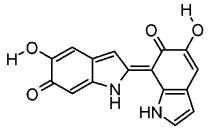

4e; vacuum (166.3°): 5.6; water (164.0°): 2.8

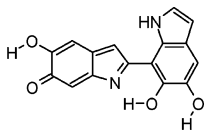

4j; vacuum (9.9°): 6.2; water (9.2°): 8.0

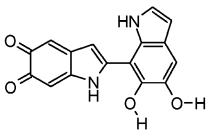

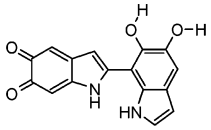

4o; vacuum (26.7°): 16.4; water (28.8°): 6.7 **4q;** vacuum (152.0°): 18.9; water (150.1°): 7.7

Figure 7. Structures and relative energies (kcal mol^{-1}) of several tautomers/conformers of **4**, computed at the PBE0/6-31+G(d,p) level in vacuo or in aqueous solution (PCM). In parentheses the inter-ring N−C−C−C(O) dihedral angle (deg) is reported.

Figure 7 presents the results of DFT computations for tautomers of **4**. Again, the extended quinone methide **4a**, featuring a 2-substituted quinone methide moiety, was the most stable tautomer, whereas the *E* isomer **4e** was disfavored by 5.6 kcal mol^{-1} in vacuo and 2.8 kcal mol^{-1} in aqueous solution. The next most stable tautomers, e.g., the 2-substituted quinone methide **4j** and the 2-substituted *o*-quinones **4q** and **4p**, were less favorable by several kilocalories per mole in aqueous solution in comparison to **4a** and are not expected to contribute to the spectrum. The picture is unaltered at the MP2/PCM level (see the Supporting Information).

The most intense bands in the electronic absorption spectra of **4a** and **4e** in aqueous solution were predicted to be around 550 nm (Table 1) and were in satisfactory agreement with the absorption maxima measured in the radiolysis experiments (Figure 4).

The nature of the electronic transitions underlying the UV−vis spectrum is similar to that for the 2,4-dimer: the main band (529 nm, $f = 0.483$, for **4a** in vacuo; 504 nm, $f = 0.499$, for **4e**) is mostly HOMO − 1 → LUMO in character, while the HOMO → LUMO (**4a**, 884 nm, $f = 0.073$; **4e**, 819 nm, $f = 0.100$) and HOMO − 2 → LUMO (**4a**, 634 nm, $f = 0.007$; **4e**, 584 nm, $f = 0.030$) transitions are much less intense. Also the basic features of the molecular orbitals are similar to those in the other asymmetric dimer, with the HOMO and to a lesser extent the HOMO − 1 mostly localized on the 7-substituted ring, while the HOMO − 2 and the LUMO are predominantly on the 2-substituted ring.

It is noteworthy that both **4a** and **4e** show a bathochromic shift of about 30 nm in their main band, with respect to the analogous tautomers **3a** and **3e**; shifts are much less prominent for the other low-energy transitions. As hinted above, the shifted

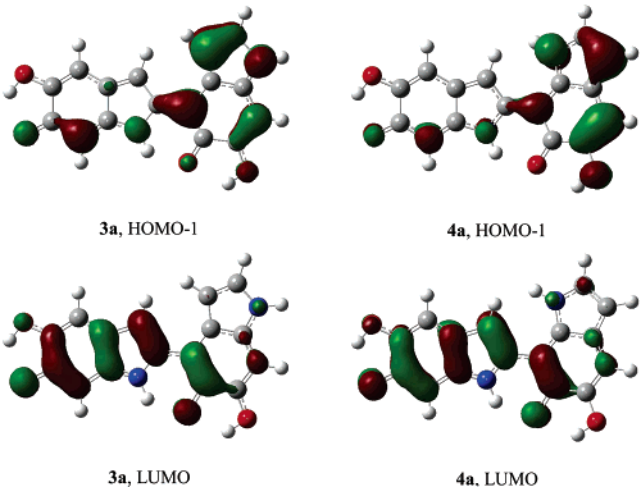

Figure 8. Isodensity surfaces (0.04 au) of selected molecular orbitals of **3a** and **4a**, computed at the PBE0/6-311++G(2d,2p)//PBE0/6-31+G(d,p) level in vacuo.

transition has a dominant HOMO − 1 → LUMO character. Figure 8 shows a comparison of the involved orbitals in **3a** and **4a**: while the LUMOs are quite similar, the HOMO − 1 molecular orbitals extend across the two rings, with significant coefficients on the nitrogen atoms of the 4- and, respectively, 7-substituted indole moieties. Therefore, it is reasonable to expect that a change in the position of the linkage may preferentially affect the energy of this orbital. The situation is perfectly parallel for **3e** vs **4e**.

From the above calculations, it is concluded that extended quinone methides are by far the most stable among biindolyl quinone tautomers. The satisfactory agreement between experimental and simulated spectra allows moreover the conclusion that the products arising from second-order decay of semiquinones are the quinones rather than tetrameric species. In the case of asymmetric dimers **3** and **4**, the most favorable among minor tautomers, in which conjugation does not extend beyond a single ring, are usually those in which the oxidized moiety is the 2-substituted indole ring.

As an additional remark, it has been noted that continuum models may fail to properly account for highly specific solute−solvent interactions (e.g., H-bonds). These interactions are apparently not crucial for the UV−vis spectra in the present case, as shown by the cluster calculations reported above. However, they could still play a relevant role in the determination of the relative stabilities of the different isomers. A systematic exploration of all water−dimeric quinone clusters would clearly be extremely expensive: therefore, we resorted to performing test cluster−PCM calculations on the parent indole quinone tautomers, whereby one water molecule from the first solvation shell is explicitly included in several possible optimized positions. The results (see the Supporting Information) indicate that the relative stability of a specific cluster is affected by the exact positioning of the explicit water molecule, but that overall the energetic trend of the different quinone tautomers is well reproduced by simple PCM computations (i.e., without explicit waters), thus corroborating the use of the continuum model to assess relative stabilities.

Isolation and Characterization of an Oxidation Product from Dimer 3. To gain experimental evidence for the involvement of extended quinone methide tautomers in dimer oxidation,

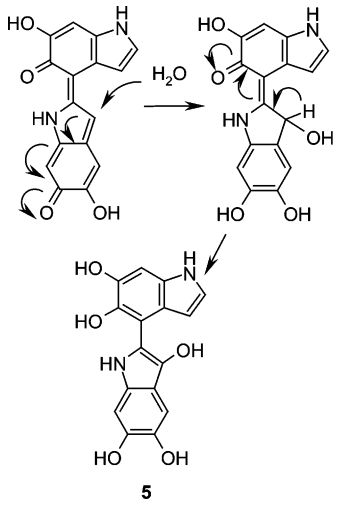

Figure 9. Proposed mechanism of formation of **5** by oxidation of dimer **3**.

in a separate set of experiments the oxidation of **3** by the HRP/H_2O_2 system in 0.05 M phosphate buffer, pH 7, was investigated. Dimer **3** was selected because of its prevalent formation in the oxidation of **1** under biomimetic conditions, which makes it a most plausible intermediate in the eumelanin pathway in vitro and in vivo. Moreover, its asymmetric structure was expected to represent a more useful probe to investigate dimer quinone reactivity and to obtain proof of the putative extended quinone methide intermediate.

TLC and HPLC analysis after acetylation and the usual workup indicated a very complex mixture of species difficult to separate. One of the products eluted under a band at R_f = 0.36 (eluant $CHCl_3$−MeOH, 98:2) proved more amenable to chromatographic isolation and was eventually obtained in minute amounts (less than 3%) for spectral characterization. The ESI^+-MS spectrum gave a pseudo molecular ion peak at *m*/*z* 545 $[M + Na]^+$, suggesting a pentaacetoxybiindolyl. Extensive 2D NMR analysis consistently indicated five acetyl groups and the lack of the H-3 proton in the 2-substituted ring. A noticeable feature of the proton NMR spectrum was an unusually downfield singlet at δ 8.20 ascribed to the H-4 proton in the 2-substituted unit experiencing the deshielding effect of the adjacent acetyl group (see Table 1S in the Supporting Information). On this basis, the product was formulated as the pentaacetyl derivative of the novel 3,5,5′,6,6′-pentahydroxy-2,4′-biindolyl (**5**).

The remainder of the reaction mixture consisted apparently of tetramers of **1** and higher oligomers (LC−MS evidence), which will form the subject of a separate study.

Although product **5** is clearly not fully representative of the complex reactivity pattern of **3** quinone, its isolation is nonetheless of interest because it reveals hitherto overlooked aspects of 5,6-dihydroxyindole oxidation chemistry remarkably predicted by theoretical calculations. Available evidence indicates that indole **1** does not tend to react through the 3-position, the only relevant precedent being the isolation of an adduct at C-3 between **1** and the antithyroid drug thiouracil.[35] However, introduction of an additional OH group in the case of **5** reflects an unexpected electrophilic reactivity of **3** quinone at the hindered 3-position of the 2-substituted indole moiety. This is possible only if that position is rendered electrophilic by a double

(35) Napolitano, A.; Palumbo, A.; d'Ischia, M.; Prota, G. *J. Med. Chem.* **1996**, *39*, 5192−5201.

bond efficiently conjugated with a carbonyl function within a planar structural moiety. Though a number of structures can be envisaged, it is noteworthy that the extended quinone methide intermediates **3a** and **3e** fulfill at best this requirement. A plausible mechanism accounting for formation of **5** is depicted in Figure 9.

Isolation of product **5** moreover corroborates the previous hypothesis[17,36] that quinones decay via reaction of the methide with water, generating hydroxylated species. This mechanism may also offer a likely explanation to the long-standing issue of oxygen incorporation during eumelanin buildup.[1,37]

Conclusions. We have provided herein the first insight into the transient intermediates generated by oxidation of 5,6-dihydroxyindole dimers and have underscored the methodological potential of chemical, pulse radiolytic, and quantum mechanical approaches when used in an integrated fashion. Spectrophotometric characterization of the species formed from pulse radiolytic oxidation and structural assignments to relevant chromophores have been carried out with the aid of a systematic computational analysis of all tautomers compatible with two-electron oxidation structures and simulation of their electronic absorption spectra. These efforts resulted in a consistent picture of tautomerization equilibria for the quinones of dimers **2**−**4** that highlighted the extended quinone methides as the most stable tautomers for all biindolyl quinones investigated. Upon oxidation, the nonplanar geometries of **2**−**4** are converted to extended quinone methide structures in which the double bond constrains the biindolyl system to an approximately planar geometry, possibly more amenable to be assembled into a stacked layer polymeric architecture. In this frame, it would also be of interest to extend calculations to the "square" dimers hypothesized by previous authors,[23b] to verify their relevance with the already considered systems, and this will be addressed in a separate study.

The isolation of pentahydroxybiindolyl **5**, an unprecedented hydroxylated indole derivative by oxidation of dimer **3**, is another important outcome of the present study. It not only provides convincing experimental evidence for the proposed generation of the extended quinone methide intermediates, but also reveals a significant difference between the oxidation chemistry of **1** and its dimers.

As far as the impact of this study on the process of eumelanin buildup in vivo is concerned, it is clear that the strictly anaerobic pulse radiolysis conditions, favoring the transient formation of high semiquinone concentrations, differ from those expected during natural melanogenesis. However, such conditions do allow sufficient amounts, not otherwise attainable, of the quinonoid products of radical disproportionation to permit their direct detection spectroscopically. It cannot be ruled out that during eumelanin synthesis in the biological environment of melanocytes other reactions may become important, such as, for example, the interaction of molecular oxygen with transient free radicals, which should be the subject of future further studies.

Experimental Section

5,6-Dihydroxyindole was synthesized as previously reported.[38] For general experimental methods and other materials see the Supporting Information.

Preparation of Dimers 2−4. A solution of **1** (300 mg, 2.0 mmol) in 0.05 M phosphate buffer (120 mL) was treated with HRP (36 U/mL) and H_2O_2 (266 μL of a 30% solution, 2.3 mmol). After 25 s of reaction time, the oxidation mixture was halted by the addition of a solution of sodium dithionite in water up to a 50 mM final concentration and worked up as reported.[14] After acetylation with acetic anhydride−pyridine overnight at room temperature the mixture was fractionated by column chromatography (gradient elution, $CHCl_3$−AcOEt from 10% to 40%) to afford **3** (70 mg, 15% yield, >90% pure) and **4** (45 mg, 10% yield, >95% pure).[14] In other experiments the reaction was carried out in acetone/0.1 M phosphate buffer, pH 7.0, 1:1, v/v, using HRP (72 U/mL) and H_2O_2 (266 μL of a 30% solution, 2.3 mmol). After 80 s of workup and fractionation of the oxidation mixture as above afforded the acetyl derivatives of dimers **3** (18 mg, 4% yield) and **4** (58 mg, 13% yield), respectively. Dimer **2** (as the *O*-acetyl derivative, 30 mg, 12% yield)[26] was obtained by oxidation of **1** (150 mg, 1.0 mmol) in 0.05 M HEPPSO buffer, pH 7.5, containing $NiSO_4 \cdot 7H_2O$ (560 mg, 2.0 mmol).

Note: Formation yields of dimers **2**−**4** are very sensitive to the reaction conditions, especially the time of oxidation of **1** and mode of addition of reagents. Isolated yields reported above are averages of at least three separate optimized preparations, with deviations not exceeding ±25%. Failure to adhere to the above protocol may result in significant variations in dimer formation yields.

Pulse Radiolysis. The pulse radiolysis experiments were performed with the 12 MeV linear accelerator at the Daresbury Laboratory, using the Free Radical Research Facility.[39] This accelerator provides pulse lengths of between 0.2 and 2 μs with doses up to 30 Gy using quartz capillary cells of optical path length 2.5 cm. Absorbed doses were determined from the transient $(CNS)_2^{\bullet-}$ formation in air-saturated potassium thiocyanate solutions (10 mM) using a G of 0.30 μM/Gy and ϵ (500 nm) = 7100 M^{-1} cm^{-1}.[40] The estimates of the molar absorption coefficients and rate constants are considered to be correct to ±15%. In a typical experiment, a solution of the appropriate indole as an acetyl derivative in methanol (15 mM) was treated under a N_2O atmosphere with a solution of 0.025 M trisodium phosphate containing 0.5 M KBr up to a 0.15 mM concentration, and after 1 min the pH of the solution was taken to 7.0 by addition of NaH_2PO_4 (0.07 M final concentration of phosphate buffer). The resulting mixture was subjected to pulse radiolysis.

Isolation of Dimer 5 as a Pentaacetyl Derivative. A solution of **3** (93 mg, 0.2 mmol) in methanol (5.0 mL) was taken under a flux of argon and treated with 0.1 M phosphate buffer, pH 12 (24.0 mL), that had prior been purged with argon. After 1 min solid KH_2PO_4 was added to pH 7.4, and peroxidase (1800 pyrogallol units) was added followed by 30% hydrogen peroxide (80 μL, 4 molar equivalents). After about 20 s the reaction was stopped by addition of a 0.2 M solution of sodium dithionite in water (4 mL) and acidified to pH 3 by addition of 2 M HCl. The mixture was extracted with ethyl acetate (3 × 30 mL), and the combined organic layers were dried over sodium sulfate and taken to dryness. The residue was acetylated with acetic anhydride−pyridine, 95:5, v/v, and fractionated by preparative TLC ($CHCl_3$/MeOH, 98:2) to give **5** as a pentaacetyl derivative (3 mg, 3% yield, R_f = 0.36): HR

(36) Lambert, C.; Land, E. J.; Riley, P. A.; Truscott, T. G. *Biochim. Biophys. Acta* **1990**, *1035*, 319−324.
(37) Nicolaus, R. A. In *Melanins*; Lederer, E., Ed.; Hermann: Paris, 1968.
(38) Benigni, J. D.; Minnis, R. L. *J. Heterocycl. Chem.* **1965**, *2*, 387−392.
(39) (a) Butler, J.; Hodgson, B. W.; Hoey, B. M.; Land, E. J.; Lea, J. S.; Lindley, E. J.; Rushton, F. A. P.; Swallow, A. J. *Radiat. Phys. Chem.* **1989**, *34*, 633−646. (b) Holder, D. J.; Allan, D.; Land, E. J.; Navaratnam, S. In *Proceedings of the 8th European Particle Accelerator Conference*; Garvey, T., Le Duff, J., Le Roux, P., Petit-Jean-Genaz, C., Poole, J., Rivki, L., Eds.; European Physical Society: Paris, 2002; pp 2804−2806.
(40) (a) Buxton, G. V.; Stuart, C. R. *J. Chem. Soc., Faraday Trans.* **1995**, *91*, 279−281. (b) Adams, G. E.; Boag, J. W.; Currant, J.; Michael, B. D. In *Pulse Radiolysis*; Ebert, M., Keene, J. P., Swallow, A. J., Baxendale, J. H., Eds.; Academic Press: London, 1965; pp 117−129.

ESI$^+$-MS *m*/*z* found 545.1156 [M + Na]$^+$, *m*/*z* calcd for $C_{26}H_{22}N_2O_{10}$-Na 545.1172. ^{1}H and ^{13}C NMR data are reported in Table 1S.

Computational Methods. All calculations were performed with the Gaussian 03 package of programs.[41] Geometries were optimized at the DFT level of theory using the PBE0 functional with the 6-31+G(d,p) basis set.[42] PBE0 (also referred to as PBE1PBE) is a hybrid functional obtained by combining a predetermined amount of exact exchange with the Perdew−Burke−Ernzerhof exchange and correlation functionals.[29] To simulate the aqueous environment, the PCM[30] was used, in combination with the UAHF parametrization for atomic radii.[43] All minima were checked by computing the harmonic vibrational frequencies. MP2/PCM single-point energies were computed with the same basis set for comparison purposes. Electronic absorption spectra of significant tautomers were estimated on the basis of excitation energy calculations using the TDDFT approach.[31] The PBE0 functional with the large 6-311++G(2d,2p) basis set was used for TDDFT computations, either in the gas phase or in solution with the PCM method. In the latter case, the linear response nonequilibrium model was used.[44] To produce graphs of computed UV−vis spectra, transitions above 190 nm were selected, and an arbitrary Gaussian line width of 50 nm was imposed.

Acknowledgment. We thank the CampusGrid of the University Federico II of Naples for computational resources. The pulse radiolysis experiments were carried out at the Free Radical Research Facility (Station 0.1) in the Synchrotron Radiation Department of the CCLRC Daresbury Laboratory, Warrington, U.K., and were financially supported by EC Grant No. 43332. We thank the Centro Interdipartimentale di Metodologie Chimico-Fisiche (CIMCF; University of Naples Federico II) for use of its NMR and mass spectrometry facilities. The technical assistance of Mrs. Silvana Corsani is gratefully acknowledged.

Supporting Information Available: General methods, NMR spectral data for dimer **5**, complete ref 41, computed UV−vis spectra of model quinone compounds, structures, relative energies, and UV−vis spectra of tautomers/conformers of **2**−**4** computed at the PBE0/6-31+G(d,p) level in vacuo or in aqueous solution, relative energies of selected tautomers/conformers of **2**−**4**, computed at the MP2/6-31+G(d,p) and PBE0/6-31+G(d,p) levels in aqueous solution (PCM), relative free energies of selected tautomers/conformers of **2**−**4**, computed at the PBE0/6-31+G(d,p) level in vacuo and in aqueous solution (PCM), transition wavelengths and oscillator strengths computed at the PBE0/6-311+G(2d,2p)/PCM//PBE0/6-31+G(d,p)/PCM level for **3a** with and without the inclusion of one explicit hydrogen-bonded water molecule at a given position, and kinetics of pulse radiolytic oxidation of compounds **2**−**4** at different wavelengths. This material is available free of charge via the Internet at http://pubs.acs.org.

JA0650246

(41) Frisch, M. J.; et al. *Gaussian 03*, Revision C.02; Gaussian, Inc.: Wallingford, CT, 2004.
(42) Francl, M. M.; Petro, W. J.; Hehre, W. J. S.; Binkley, J.; Gordon, M. S.; DeFrees, D. J.; Pople, J. A. *J. Chem. Phys.* **1982**, *77*, 3654−3665. For a general introduction to basis sets see: Foresman, J. B.; Frisch, A. *Exploring Chemistry with Electronic Structure Methods*, 2nd ed.; Gaussian, Inc.: Pittsburg, PA, 1996.
(43) Barone, V.; Cossi, M.; Tomasi, J. *J. Chem. Phys.* **1997**, *107*, 3210−3221.
(44) Cossi, M.; Barone, V. *J. Phys. Chem. A* **2000**, *104*, 10614−10622.